Journal of Avian Biology

JAV-01096
Cooper, N. W., Hallworth, M. T. and Marra, P. P. 2016. Light-level geolocation reveals wintering distribution, migration routes, and primary stopover locations of an endangered long-distance migratory songbird. – J. Avian Biol. doi: 10.1111/jav.01096

Supplementary material

Appendix 1 {Full details of light-level analysis}

We analyzed light-level data under a Bayesian framework using the Solar/Satellite Geolocation for Animal Tracking (SGAT) package (Wotherspoon et al., 2013 b) for program R (R Core Team 2016). SGAT uses Markov Chain Monte Carlo (MCMC) simulations to estimate positions and quantify the error inherent in light-level geolocation. SGAT requires; 1) a sensible set of estimated positions to begin sampling (i.e., a logical prior), 2) a twilight error distribution that models error in sunrise/sunset determination, and 3) a behavioral model incorporating a distribution of probable flight speeds. It also allows inclusion of spatial probability masks, which make certain locations more or less likely based on the study species' behavior. Below, we discuss our methods for each part of this process in detail.

Initial data download and processing

We first downloaded light-level data from the devices using BASTrack software (British Antarctic Survey). One device showed a clock drift of greater than two minutes and was adjusted accordingly. We then used package "BAStag" (Wotherspoon et al., 2013 a) to derive twilight times using the threshold-method (Hill & Braun, 2001). We used a light intensity threshold of one for all individuals. In contrast to many studies (reviewed by Bridge et al., 2013), we did not manually edit or discard twilights except for extremely obvious cases such as a few instances in which sunrise appeared to occur during the middle of the night, possibly due to geolocator error or anthropogenic light sources. Bridge et al., (2013) argued that visual inspection and discarding of outliers is an inherently subjective process that inhibits reproduction of results.

Creating a logical prior

To create a logical prior to begin sampling, we used functions with SGAT to estimate geographic position from the light-level data. However, to determine geographic location from light-level data, an appropriate zenith angle must first be estimated. The zenith angle is defined as the angle of the sun, in relation to the 90° vertical axis of the earth, at which the light level determined by the geolocator crosses a specified light threshold (in our case threshold = 1). To determine an appropriate zenith angle, light-level analyses require a calibration period at a known location (Lisovski et al., 2012). We used the period from geolocator deployment on the breeding grounds until July 25th because we knew all males were still on their breeding territories until this time. The zenith angle we estimated varied by individual but ranged from 95.3° to 95.9°. We then used this zenith angle for the entire year to plot estimated positions.

Upon close inspection of our data, we noticed that following the vernal equinox, when males should be essentially stationary on the wintering grounds (Bocetti et al., 2014), our initial location estimates indicated that prior to the beginning of spring migration, most males made sustained northwards movements several hundred kilometers into the open ocean, which did not make biological sense (Fig. 1a below). This indicated to us that assuming the same zenith angle for the breeding and wintering periods was incorrect (see also Hallworth et al. 2015). Determining the exact zenith angle for periods outside of a calibration period is not possible, and the zenith angle may vary depending upon shading due to weather, terrain, and vegetation (Lisovski et al., 2012). Using an inappropriate zenith angle will produce biased estimates of position and the amount of bias increases near the equinox (Lisovski et al., 2012). To estimate the zenith angle during the wintering period, we iteratively increased the zenith angle for the wintering period by 0.1° until all wintering period position estimates (i.e., before and after vernal equinox) visually converged upon a

single latitude (Fig. 1b below). Zenith angles for the wintering grounds were increased by 0.2° to 1.8° from the breeding zenith angle, resulting in a range of wintering zenith angles from 95.9° to 97.5°. We then averaged the breeding and wintering zenith angles for each bird as an estimate of the zenith angle during the migration period, though using just the breeding or wintering angle for the migration period did not greatly affect position estimates (e.g., Fig. 2 below). Estimation of latitude surrounding the autumnal and vernal equinoxes is difficult because of low variation in day length (Lisovski et al., 2012) and therefore we did not directly estimate positions 21 days before and after each equinox. Instead we assumed a linear progression of positions between the estimated positions just prior to and immediately following the equinox periods to provide a starting point for further MCMC simulations.

The twilight error distribution

To create a twilight error distribution we compared our estimated sunrise and sunset times during the calibration period with the sunrise and sunset times predicted for each bird's known breeding location. The difference between estimated and predicted twilight times during the calibration period was modeled using a log-normal distribution and assumed to reflect error in twilight estimation throughout the rest of the year (Lisovski et al., *In Press*).

The behavioral model

The behavioral model defined speed relative to the ground (i.e., ground speed), and was assumed to follow a gamma distribution ($k = 0.7$, $\theta = 0.08$). We assumed that the maximum speed was ~50 km/hr (Pennycuick et al., 2013), but that the most probable speed was below one because

Kirtland's Warblers spend most of the year stationary on either the breeding grounds or wintering grounds.

Creating the spatial probability mask

We initially created a spatial probability mask that defined positions on land as being much more likely than positions over water. However, given the fairly large error inherent in light-level geolocation and the large landmass of Cuba, this resulted in all males showing a high probability of wintering in Cuba even though initial position estimates based solely on light-levels indicated only one bird wintered in Cuba. As a result, we treated 300 km around all landmasses in the Caribbean as land to avoid this problem. Positions with increasing distance (up to 100 km) from the shoreline in the Atlantic Ocean, outside of the Caribbean, and also in the Gulf of Mexico were treated as unlikely but not impossible. Our spatial probability mask also did not allow for positions above 51°N (southern tip of Hudson Bay, Canada) or below 15°N (south of Jamaica and Hispaniola). This conservative assumption was based on sighting data (Petrucha et al., 2013) and only affected positions estimated during the equinox periods.

MCMC Sampling

Using our logical prior, twilight error distribution, flight speed model, and spatial probability mask, we then used the Metropolis-Hastings sampler within SGAT to draw 120,000 samples for burn-in and tuning, and a final 15,000 samples to define the posterior distribution, where each sample represented one set of estimated locations. Three independent chains were used for each part of the process so that we could visually assess chain convergence. For several males, the chains did not converge and therefore we doubled the number of samples for burn-in and tuning until chains

visually converged. To estimate location error, we compared the locations from the mean path from all 15,000 iterations during the calibration period with the known breeding location and found that location error was 77 ± 46.4 km ($\bar{x}$ ± S.D.) during this period.

Defining the wintering distribution

Using position estimates drawn from posterior distribution, we defined the wintering range for each male as the 95th quantile of all positions from 15 November until 21 days prior to the vernal equinox. To describe the wintering distribution of all males, we combined individual wintering ranges into a single raster.

Defining migration timing and distance

We estimated the dates each bird departed on fall and spring migration and arrived on the wintering and breeding grounds. For each bird, we first defined the most likely movement path as the mean position of all 15,000 iterations. For the purpose of determining departure and arrival dates, we spatially defined each bird's breeding range as the 95th quantile of all positions from deployment until 21 days prior to the autumnal equinox, and the wintering range as the 95th quantile of all positions from November 15th until 21 days prior to the vernal equinox. Latitudinal, but not longitudinal, estimates are unreliable during the period surrounding the equinoxes, and so we defined fall departure date as the first day the mean path moved eastward outside of the breeding range, without return (Hallworth et al., 2015). Arrival date on the wintering grounds was defined as the first day each bird's mean path entered, without exiting, the wintering range. We defined spring departure date from the non-breeding grounds as the first day each bird's estimated path left the wintering range, without return. We used the first day each males' mean path entered the breeding

range, without exiting, as its spring arrival date. We defined "fall jump off" as the last day each bird's mean path remained on land before crossing into the Atlantic Ocean. We defined spring landfall as the first day each bird's mean path crossed into the continental United States. For each male we estimated spring migration distance by determining the shortest distance between successive points along each bird's mean path. When determining migration distance, we assumed that males were stationary at the centroid of each stopover area for the duration of each stopover period. This prevented inclusion of movement that was simply due to inherent error in position estimation using light-level data and provides a more accurate estimation of migration distance. Fall migration distance could not be accurately estimated because stopover periods could not be determined due to the autumnal equinox.

Estimating stopover locations

To determine stopover periods during migration, we first transformed the positions from each bird's mean path back into twilight times. Then we used the "changeLight" function within package "GeoLight" (Lisovski and Hahn 2013) to determine large changes (i.e., change-points) in twilight times to estimate when birds moved. This process however, can be influenced by shading events. Therefore, we set a transition probability of 0.95 and a minimum stopover duration of one day to minimize identification of false movements. This process worked well for spring migration but failed to identify change-points in the light data during fall migration due to the uncertainty of latitude during the equinox period. For fall migration, we were only able to qualitatively identify stopover regions using time spent maps produced in SGAT. Time spent maps indicate the probability of residency relative to the period of inquiry. For each male, we created a time-spent map of the fall migration period to indicate where males spent the most time on fall migration. We

then combined the 95th quantile of positions during fall migration for all males into a single raster to identify potentially important stopover areas. Spring migration was not overlapped by the vernal equinox and thus we were able to estimate the number, duration, and general location of each stopover made during spring migration.

Figure 1. Daily latitudinal estimates for one male Kirtland's Warbler (*Setophaga kirtlandii*) for one year using (a) the same zenith angle for breeding and wintering periods and (b) different zenith angles for breeding and wintering periods. The solid horizontal line indicates the known breeding latitude. Dashed vertical lines indicate the autumnal and vernal equinox.

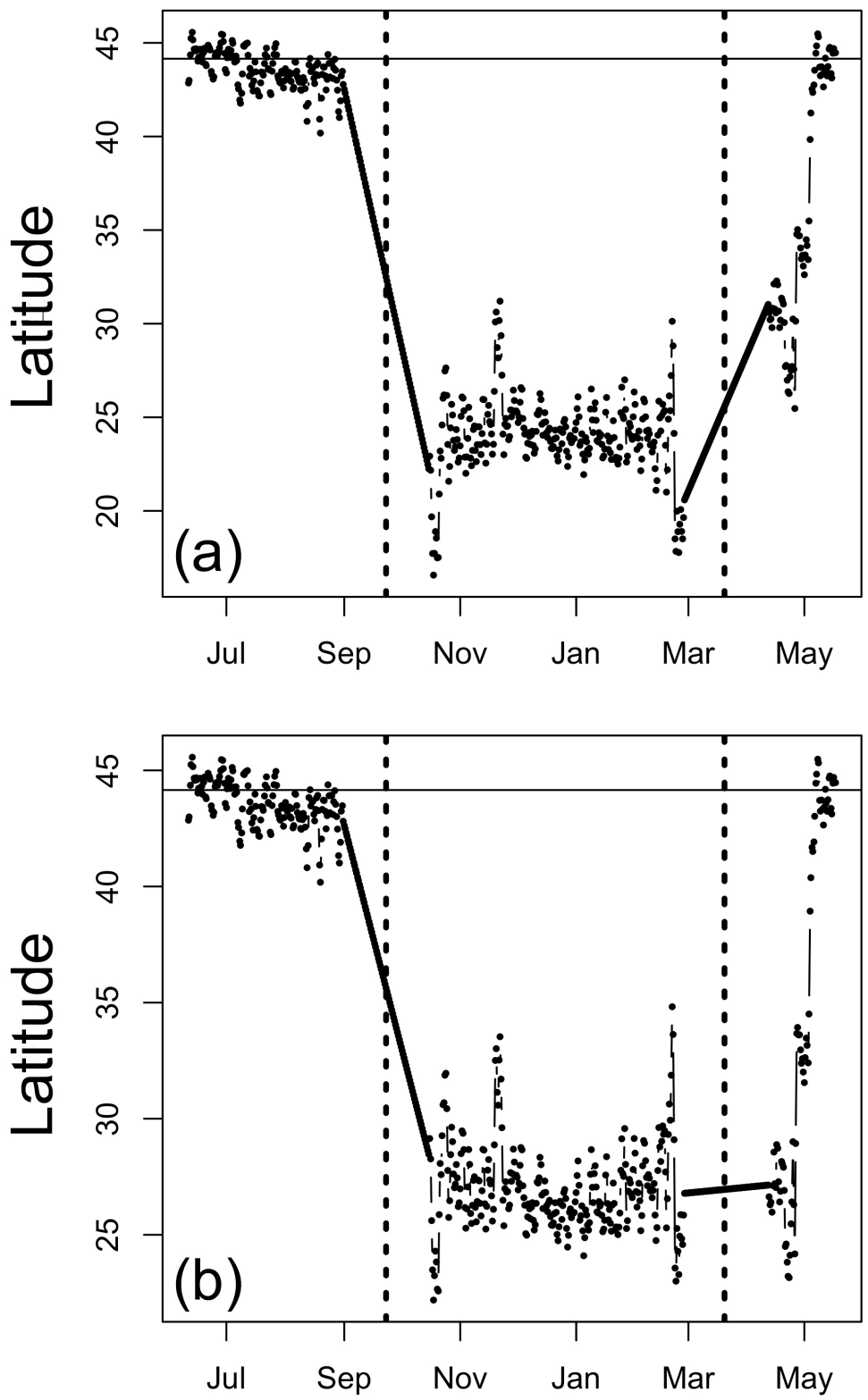
Latitude
45
40
35
30
25
20
(a)
Jul
Sep
Nov
Jan
Mar
May
Latitude
45
40
35
30
25
(b)
Jul
Sep
Nov
Jan
Mar
May

Figure 2. Relative probability of residency of one male Kirtland's Warbler (*Setophaga kirtlandii*) for one year. Probability of residency increases from peach to blue. The outer bounds of the colored area represent the lowest probability positions. Red, green, and black lines represent spring migration when breeding, wintering, or average zenith angles were used to produce position estimates.

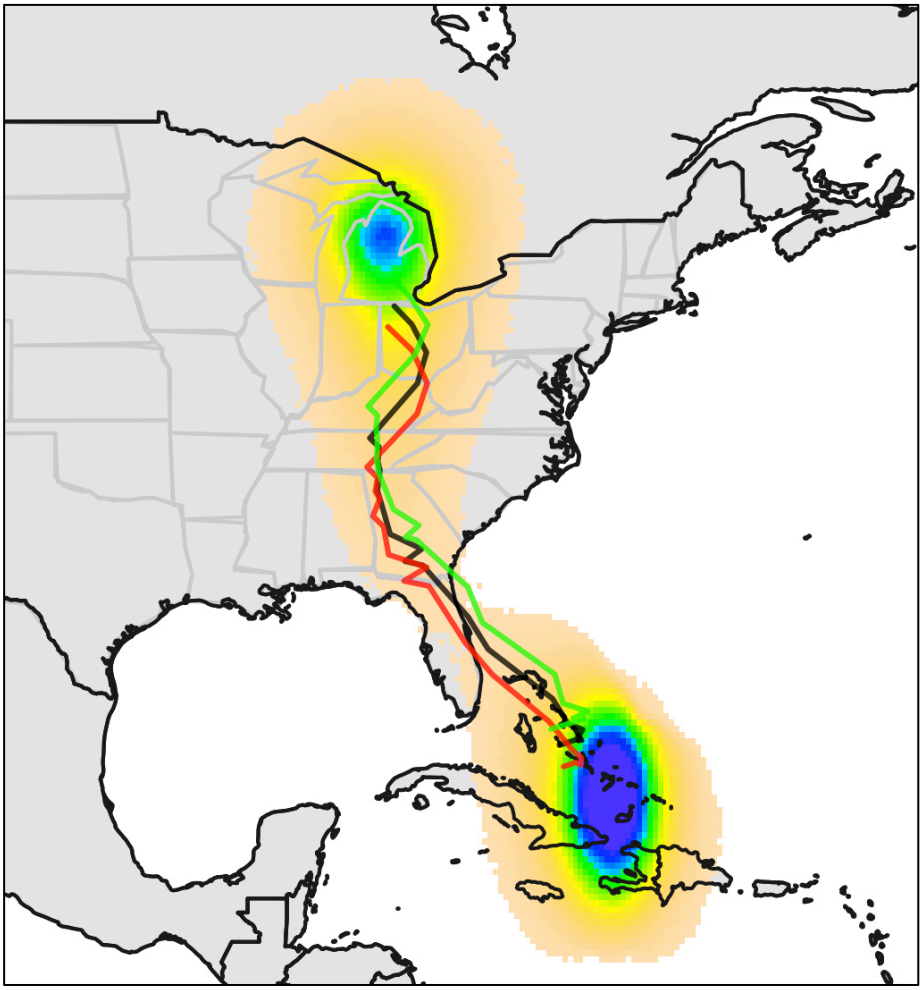

References

Bocetti, C.I., D.M. Donner, & H.F. Mayfield. (2014) Kirtland's Warbler (*Setophaga kirtlandii*). *The Birds of North America Online* (ed. by A. Poole). Cornell Lab of Ornithology, Ithaca.

Bridge, E.S., J.F. Kelly, A. Contina, R.M. Gabrielson, R.B. MacCurdy, & D.W. Winkler. (2013) Advances in tracking small migratory birds: a technical review of light-level geolocation. *Journal of Field Ornithology*, **84**, 121-137.

Hallworth, M.T., T.S. Sillett, S.L. Van Wilgenburg, K.A. Hobson, & P.P. Marra. (2015) Migratory connectivity of a Neotropical migratory songbird revealed by archival light-level geolocators. *Ecological Applications*, **25**, 336-347.

Hill, C., & M.J. Braun. (2001) Geolocation by light level - the next step: latitude. *Electronic tagging and tracking in marine fisheries* (ed. by J.R. Sibert and J. Nielson), pp. 315-330. Kluwer Academic Publishers, The Netherlands.

Lisovski, S., & S. Hahn. (2012) GeoLight - Processing and analysing light-based geolocator data in R. *Methods in Ecology and Evolution*, **3**, 1055-1059.

Lisovski, S., C.M. Hewson, R.H.G. Klaasen, F. Korner-Nievergelt, M.W. Kristensen, & S. Hahn. (2012) Geolocation by light: accuracy and precision affected by environmental factors. *Methods in Ecology and Evolution*, **3**, 603-612.

Lisovski, S., K. Gosbell, C. Maureen, B. Hoye, M. Klaasen, I. Stewart, A. Taysom, & C. Minton. (*In Press*) Movement patterns of Sanderling (*Calidris alba*) along the East Asian Australasian Flyway and a comparison of methods to identify crucial areas for conservation. EMU - Austral Ornithology.

Pennycuick, C.J., S. Åkesson, & A. Hedenström. (2013) Air speeds of migrating birds observed by ornithodolite and compared with predictions from flight theory. Journal of the Royal Society Interface, **10**, 20130419.

Petrucha, M.E., P.W. Sykes Jr., P.W. Huber, & W.W. Duncan. (2013) Spring and fall migrations of Kirtland's Warbler (*Setophaga kirtlandii*). *North American Birds*, **66**, 382-427.

R Core Team. (2016) *R: A language and environment for statistical computing*. R Foundation for Statistical Computing, Vienna.

Wotherspoon, W., M. Sumner, and S. Lisovski. (2013 a) BAStag: Basic data processing for light based geolocation archival tags. R package version 0.1-3.

Wotherspoon, S.J., M.D. Sumner, & S. Lisovski. (2013 b) R Package SGAT: Solar/Satellite Geolocation for Animal Tracking. GitHub Repository [https://github.com/SWotherspoon/SGAT].